Efficient Path Following Algorithm for Unmanned Surface Vehicle

Conference Paper · April 2016

DOI: 10.1109/OCEANSAP.2016.7485430

4 authors, including:

Al Savvaris
Cranfield University
106 PUBLICATIONS **2,651** CITATIONS

SEE PROFILE

Antonios Tsourdos
Cranfield University
734 PUBLICATIONS **9,337** CITATIONS

SEE PROFILE

Efficient Path Following Algorithm for Unmanned Surface Vehicle

Hanlin Niu
School of Aerospace, Transport and Manufacturing
Cranfield University
Bedford, United Kingdom
h.niu@cranfield.ac.uk

Yu Lu
School of Aerospace, Transport and Manufacturing
Cranfield University
Bedford, United Kingdom
Yu.lu.2@cranfield.ac.uk

Al Savvaris
School of Aerospace, Transport and Manufacturing
Cranfield University
Bedford, United Kingdom
a.savvaris@cranfield.ac.uk

Antonios Tsourdos
School of Aerospace, Transport and Manufacturing
Cranfield University
Bedford, United Kingdom
a.tsourdos@cranfield.ac.uk

***Abstract*— This paper presents the comparison and analysis of four common path following algorithms for the C-Enduro unmanned surface vehicle (USV), which is designed to operate at sea for extended periods of time (up to 3 months). Four path following algorithms were tested that include Carrot chasing path following, Nonlinear guidance law, Pure pursuit and line-of-sight (PLOS) path following and Vector field algorithms. The simulation was realized by implementing the 3 DOF dynamic model of C-Enduro USV. The simulation also took account of the environmental factors, i.e., wind and current. The accuracy and control effort of these four algorithms are compared and analyzed. The simulation results can be used to assist in deciding which path following algorithm the USV needs to implement in order to deal with different missions efficiently.**

Keywords*— *Unmanned marine vehicles; Long endurance; Path following; Marine system navigation, guidance and control.

I. ASV VEHICLE DESCRIPTION

The C-Enduro USV was developed under a UK Government-backed Small Business Research Initiative (SBRI) initiated by the National Oceanography Centres (NOC) requirement for long endurance USVs for environmental research. The team behind the C-Enduro, led by ASV whom built and integrated the systems of the vessel, includes Hyperdrive Ltd who investigated motor options and power management systems and Cranfield University who have conducted research into collision avoidance technologies [1]. The development of collision avoidance algorithm algorithms for the C-Enduro was presented in [2].

Fig. 1. The C-Enduro Unmanned Surface Vehicle

Fig.1 shows a picture of the C-Enduro unmanned marine surface vehicle out at sea.

To meet the requirement of long endurance capability, the C-Enduro vehicle has a 'three pillar' energy system that includes solar panels, a wind generator and a diesel generator. Calculations and tests show that this 'three pillar' energy system, combined with efficient power management and command and control systems packaged in a rugged self-righting vehicle, provides the greatest likelihood of meeting the performance requirement. Table 1 shows the physical technical specification and table 2, which is provided by ASV Ltd [3], shows the technical specifications of the wind generator, diesel generator and the solar panel.

Table 1. Physical Technical Specification

Physical	Specification
Length	4.2m
Beam	2.4m (road transportable)
Height	2.8m (including antenna), 1.5m (mast off)
Draft	0.4m
Weight	350kg (lightship)
Primary propulsion	2 DC brushless motors

In terms of the power system hardware, the C-Enduro USV has the right ingredients to be a successful long endurance vessel. Moreover, from software aspect, to improve the endurance capacity and the capability to follow a path accurately, four path following algorithms were compared and analysed in order to provide the guidance system the proper path following algorithms for different mission scenarios. These four path following algorithms include Carrot chasing path following, Nonlinear guidance law, Vector field algorithms and PLOS path following.

978-1-4673-9724-7/16/$31.00 ©2016 European Union

Table 2. Power and Controls Technical Specification

Power and controls	Specification
Endurance	Up to 3 months utilizing solar/wind/diesel energy.
Speed	0-7 knots operational speed range
Navigation aids	GPS, AIS, Navigation Lights
Solar panel system	Generating a peak electrical power of 1200W
Diesel generator system	Providing a peak charging power of 2.5kW
Wind turbine system	Lightweight three blade system generating a peak output power

Since the C-Enduro USV is designed to be capable of avoiding obstacles and travel long distances efficiently, the control effort and cross track error were chosen as the criteria of evaluating the performance of the four path following algorithms.

II. PATH FOLLOWING LITERATURE REVIEW

A large number of USV missions are straight line following and circular path following. The distance between the vehicle position and the predefined path is called cross-track error. The requirements of the path following algorithm are to reduce the cross-track error and minimize the difference between the vehicle course angle and the predefined course angle.

The path following algorithms can be divided into two categories: geometric algorithms and control theory based algorithms. The geometric algorithms are mostly simple to implement. A common geometric algorithm is Carrot Chasing algorithm. The Carrot Chasing algorithm is to apply a virtual target point (VTP) on the path, when the vehicle is chasing the VTP, it will follow the path. Carrot chasing algorithm has been tested in [4]. Another path following method that is similar to Carrot Chasing algorithm is called nonlinear guidance law (NLGL) and [5] has proved the Lyapunov stability of NLGL. Nonlinear guidance law also uses VTP concept but the VTP is the intersection between the circle that is around the USV and the predefined path. The other geometric algorithms include Line-of-Sight (LOS) algorithm, pure pursuit and combination of pure pursuit and LOS (PLOS). These three algorithms have been proved in [6], [7] and [8], respectively. Some of the control theory based algorithms are PID based path following algorithm, Lyapunov vector field method, linear quadratic regulator (LQR) and adaptive control method. The PID based path following algorithm has been demonstrated in [9], linear quadratic regulator was proved in [10] and adaptive control method was presented in [11]. The vector field method principle is to use vector field to generate the flow direction, let the vehicle follow the vector field direction and the vehicle will follow the path. The Lyapunov stability argument has been demonstrated in [12]. The linear quadratic regulator also takes account of the control error to drive the vehicle to follow the path and it minimizes the control effort to reduce the cross track error.

This paper not only test one USV path following geometric algorithm but evaluate four common path following algorithms to show the performance of cross track error and control effort in the existence of current and wind disturbances. The simulation results can be used to assist in deciding which path following algorithms the USV need to implement to deal with different missions requirements efficiently.

III. USV 3 DOF MODEL AND CONTROL SYSTEM

In this section, the C-Enduro USV 3 DOF dynamic model and control system are introduced.

A. C-Enduro USV 3-DoF Model

Due to the fact that the two thrusters of the C-Enduro vessel are the two fixed pitch propellers on the left and right hull and the vessel has no rudder and fins on it, the control of the thrusters can only manoeuvre planar motions including surge, sway and yaw. Thus, the C-Enduro model is designed to be 3 DoF planar model neglecting heave, pitch and roll dynamics.

The vehicle is also assumed to be both right-left and fore-after symmetric. By simplifying 6 DoF dynamics and kinematics equations of motion in [13], the 3 DoF model can be given as follows:

$$\dot{\eta} = J(\eta)\nu \quad (1)$$

$$M\dot{\nu} + C(\nu)\nu + D(\nu)\nu + g(\eta) = \tau_E + \tau \quad (2)$$

$$M = M_{RB} + M_A \quad (3)$$

$$C(\nu) = C_{RB}(\nu) + C_A(\nu) \quad (4)$$

where

$$\eta = [x, y, \psi]^T$$

$$\nu = [\mathrm{u}, \mathrm{v}, \mathrm{r}]^{\mathrm{T}}$$

$J(\eta) =$ transformation matrix between the body coordinate and the earth-fixed coordinate system

$M =$ inertial matrix (including added mass M_A)

$C(\nu) =$ matrix of Coriolis and centripetal terms (including added mass $C_A(\nu)$)

$M_{RB} =$ rigid-body inertia matrix

$C_{RB}(\nu) =$ rigid-body coriolis and centripetal matrix

$D(\nu) =$ damping matrix

$g(\eta) =$ vector of gravitational forces and moments

$\tau_E =$ environmental forces and moments (including current, waves and wind)

$\tau =$ propulsion forces and moments

B. Control System

The speed and course angle are controlled by a PI speed controller and a PD heading controller, respectively. Due to the page limit of this paper, the derivation of the controller design will be abbreviated. The speed controller gain K_p and K_d can be calculated by (5) and (6).

$$k_p = X_u + 2X_{|u|u}u_0 + 2(m - X_{\dot{u}})\sigma \quad (5)$$

$$k_i = (m - X_{\dot{u}})(\sigma^2 + \omega_n^2) \quad (6)$$

The desired speed is denoted by u_0 and the mass of the boat is denoted by m. $X_{\dot{u}}$ is the added mass factor and $X_{|u|u}$ is the damping factor.

The course angle controller gain K_p and K_d can be calculated using (7) and (8).

$$K_p = \frac{T\omega_n^2}{K} \quad (7)$$

$$K_d = \frac{2T\zeta\omega_n - 1}{K} \quad (8)$$

T is the time constant and K is the gain constant. ω_n is the natural frequency and ζ is the relative damping ratio, which can be treated as design parameters.

IV. PATH FOLLOWING ALGORITHMS

The principles of Carrot chasing path following, Nonlinear guidance law, PLOS path following and Vector field algorithms are introduced in this section. For all the algorithms below, the USV positions are all denoted as $p\,(x, y)$, the course angle of USV is denoted as ψ and the speed of the USV is v.

A. Carrot Chasing Algorithm

Carrot chasing (CC) path following algorithm is one of the most widely used and easy to implement. To follow a predefined path, a virtual target point (VTP) is introduced on the path. The USV will always follow the VTP and the VTP is called carrot, hence, this algorithm is called carrot chasing algorithm.

In Fig.2, the straight line is represented by using the line between two waypoints W_i and W_{i+1} The USV position is denoted by $p\,(x, y)$ and the course angle is denoted by ψ. The projection of p on line AB is q. The distance between p and q is denoted by d. The VTP is denoted as s. The distance between q and s is δ, which needs to be defined by the user.

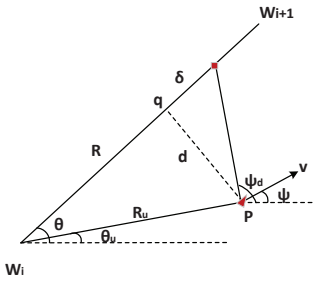

Fig. 2. Carrot chasing straight line following algorithm

The equations are given as follows:

$$R_u = \|W_i - p\| \quad (9)$$

$$\theta = \text{atan}\left(\frac{y - y_i}{x - x_i}\right) \quad (10)$$

$$\beta = \theta - \theta_u \quad (11)$$

$$R = R_u \cos(\beta) \quad (12)$$

Then, the position of VTP $s\,(x_t, y_t)$ is given by:

$$x_t = (R + \delta)\cos(\theta) \quad (13)$$

$$y_t = (R + \delta)\sin(\theta) \quad (14)$$

The desired course angle ψ_d is given by:

$$\psi_d = \text{atan}\left(\frac{y_t - y}{x_t - x}\right) \quad (15)$$

The desired course angle turning rate $\dot{\psi}$ is given by:

$$\dot{\psi} = \frac{\psi_d - \psi}{\Delta t} \quad (16)$$

When the USV is following the predefined path, the path following algorithm is calculating in a loop. Firstly, calculate out the cross track error d. Secondly, update the VTP position. Finally, update ψ_d and $\dot{\psi}$.

B. Nonlinear Guidance Law

The Nonlinear guidance law (NLGL) is also using the concept VTP for the USV to follow. However, unlike carrot chasing that uses a configured value δ or λ to make the USV move forward, NLGL is using the intersection between a given radius circle around the USV position and the predefined path as the position of VTP.

The geometry of NLGL straight line following is shown in Fig.3. $p(x, y)$ is the position of the USV. The given radius of the USV circle is denoted by L. The two intersections between the circle and the straight line are noted as s and s′. The positions of the two waypoints W_i and W_{i+1} are denoted as (x_i, y_i) and (x_{i+1}, y_{i+1}).

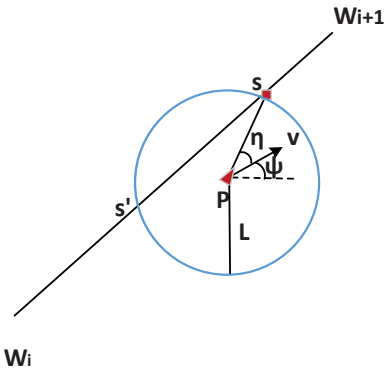

Fig. 3. NLGL straight line following algorithm

The following two equations will give the two intersections position solutions. Assume the VTP position is denoted by $s(x_t, y_t)$.

$$(x_t - x)^2 + (y_t - y)^2 = L^2 \quad (17)$$

$$y_t = \frac{y_{i+1} - y_i}{x_{i+1} - x_i} x_t - \frac{y_{i+1} - y_i}{x_{i+1} - x_i} x_i + y_i \quad (18)$$

There will be two solutions for $s(x_t, y_t)$, the one which is near to W_{i+1} is the VTP. By calculating the line-of-sight angle from USV position $p\,(x, y)$ to $s(x_t, y_t)$, we get the desired course angle ψ_d.

$$\psi_d = \text{atan}\left(\frac{y_t - y}{x_t - x}\right) \quad (19)$$

Then, the desired course angle turning rate is given by.

$$\dot{\psi} = \frac{\psi_d - \psi}{\Delta t} \tag{20}$$

C. Vector Field Algorithm

The principle of vector field (VF) path following is that the unmanned vehicles will follow the direction of the vector field. The vector field path following method can be used for straight following and loiter. Lyapunov stability arguments are applied to demonstrate the stability of VF path following algorithm that was presented in [12].

An example of VF straight line following was carried out in Matlab, Fig.4 shows the principle of VF straight line following algorithm.

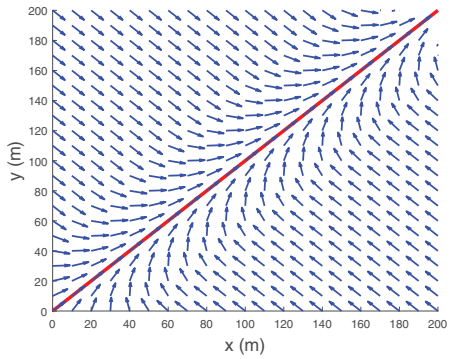

Fig. 4. Vector Field straight line path following

In Fig.4, the red line represents the predefined path and the blue arrows represent the vector field direction. The principle of the vector field straight line following algorithm is that when the vehicle is inside the boundary τ that is close to the predefined path, the desired course angle will be updated to following the path. When the vehicle is far away from the path, the vehicle will move perpendicular to the path until it moves into the boundary.

The equations used for deriving the desired course angle turning rate are given below:

The line-of-sight angle of the straight path is denoted by θ.

$$\theta = atan\frac{y_{i+1} - y_i}{x_{i+1} - x_i} \tag{21}$$

$$s^* = \frac{(p - W_i)^T (W_{i+1} - W_i)}{\|W_{i+1} - W_i\|^2} \tag{22}$$

$$\varepsilon = \|p - (s^*(W_{i+1} - W_i) + W_i)\| \tag{23}$$

$$\rho = sign[(W_{i+1} - W_i) \times (p - W_i)] \tag{24}$$

$$\varepsilon = \rho\varepsilon \tag{25}$$

There are two situations when the vehicle is inside the boundary or outside.

When the vehicle is inside the boundary τ,

$$\psi_d = \theta - \rho\chi^e \tag{26}$$

When the vehicle is outside the boundary τ,

$$\psi_d = \theta - (\chi^e)\left(\frac{\varepsilon}{\tau}\right)^k - \left(\frac{k\chi^e v_a}{\alpha\tau^k}\right)\varepsilon^{k-1} sin\psi \tag{27}$$

In these equations, χ^e, k and τ should be defined by the users. The higher χ^e is, the quicker the USV will move toward the LOS line. If χ^e is small, the cross track error will also be large.

D. Pure Pursuit and LOS Path Following

Pure pursuit and line-of-sight (PLOS) path following is a combination between pure pursuit guidance and line-of-sight guidance laws. It not only drives the USV to the destination using pure pursuit guidance laws but also minimizes the cross error d using LOS guidance. The algorithm of PLOS straight line following is given below.

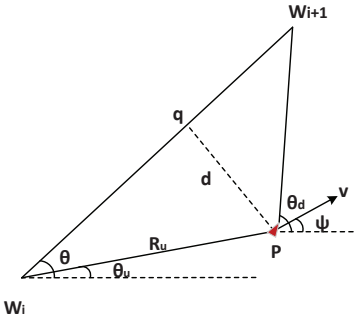

Fig. 5. PLOS straight line path following

The line-of-sight angle between USV position p (x, y) and the destination W_{i+1} is denoted by θ_d.

$$\theta_d = atan\frac{y_{i+1} - y}{x_{i+1} - x} \tag{28}$$

$$d = \frac{(y_i - y_{i+1})x + (x_{i+1} - x_i)y + (x_i y_{i+1} - x_{i+1} y_i)}{\|W_i - W_{i+1}\|} \tag{29}$$

$$\psi_d = k_1(\theta_d - \psi) + k_2 d \tag{30}$$

k_1 and k_2 are two weighted factors that should be defined by the users. Then, the desired course angle turning rate can be calculated out.

$$\dot{\psi} = \frac{\psi_d - \psi}{\Delta t} \tag{31}$$

V. SIMULATION RESULTS

In this section, the performances of the path following algorithms are compared under two situations. The first situation is when there is no wind and no current. The second situation is when there are both wind and current disturbances.

In the first case, the wind speed V_w and the current speed V_c were assumed to be $0\ m/s$. The initial heading angle was assumed to be true north. The predefined path was from (0,0) to (1000,1000). The USV initial position was assumed to be (0,0), the initial heading angle is assumed to be $90^o$and the USV was assumed to travel at constant speed. The simulation duration was 500 seconds. The parameters of each algorithm are given in table 3.

Table 3. Path following parameters

Carrot Chasing (CC)	Nonlinear Guidance (NLGL)	Vector Field (VF)	Pure pursuit and LOS (PLOS)
$\delta = 10$	$L = 15$	$\chi^e = \frac{\pi}{2}$ $\tau = 35$ k = 1 $\alpha = 20$	$k_1 = 1$ $k_2 = 0.1$

The simulation results of the first case are shown in Fig. 6 to Fig. 9.

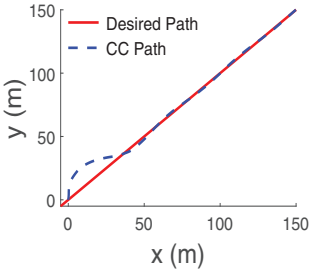

Fig. 6(a). CC Path

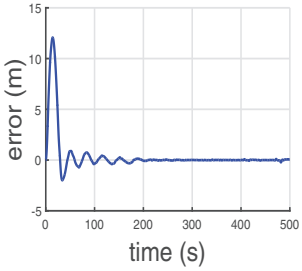

Fig. 6(b). CC cross track error

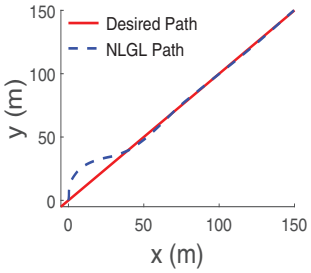

Fig. 7(a). NLGL path

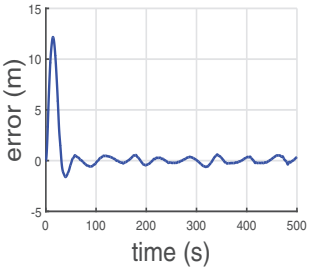

Fig. 7(b). NLGL cross track error

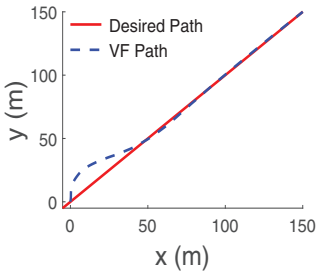

Fig. 8(a). VF path

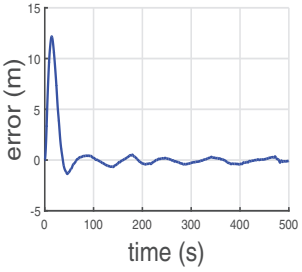

Fig. 8(b). VF cross track error

From Fig.6(b) and Fig.9(b), we can see that the tracking error of Carrot Chasing algorithm and PLOS algorithm oscillated at the start and then converging to zero. However, the tracking error of Nonlinear guidance law and vector field did not converge to zero.

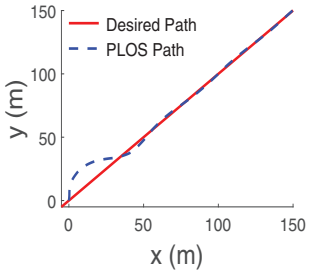

Fig. 9(a). PLOS path

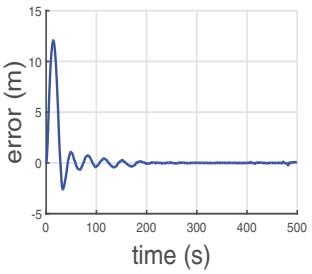

Fig. 9(b). PLOS track error

In the second case, both wind and current disturbances are taken into account. The wind speed V_w is assumed to be 3 m/s and the sea current speed V_c is assumed to be 0.2 m/s. The wind and sea current directions are assumed to be 270^o. The performance of the four path following algorithms are given below.

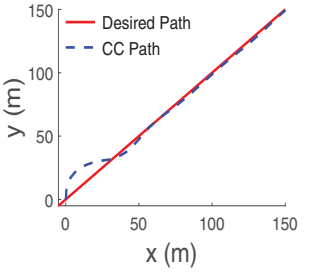

Fig. 10(a). CC path

$(V_w = 3m/s, V_c = 0.2m/s)$

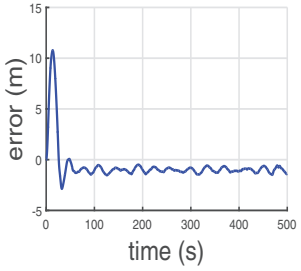

Fig. 10(b). CC cross track error

$(V_w = 3m/s, V_c = 0.2m/s)$

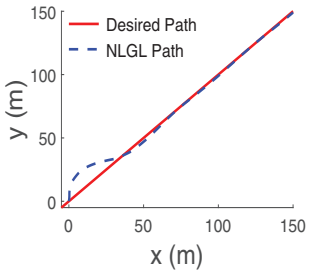

Fig. 11(a). NLGL path

$(V_w = 3m/s, V_c = 0.2m/s)$

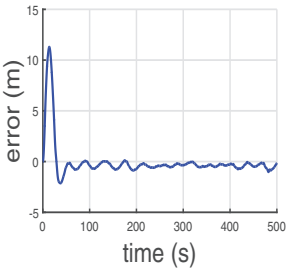

Fig.11(b). NLGL cross track error

$(V_w = 3m/s, V_c = 0.2m/s)$

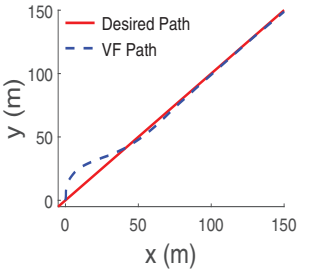

Fig. 12(a). VF path

$(V_w = 3m/s, V_c = 0.2m/s)$

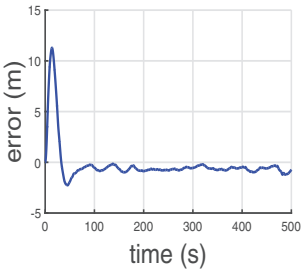

Fig. 12(b). VF cross track error

$(V_w = 3m/s, V_c = 0.2m/s)$

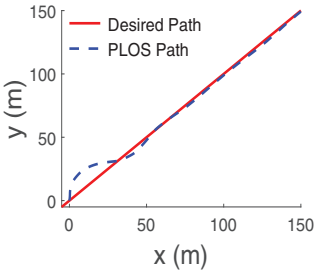

Fig. 13(a). PLOS path

$(V_w = 3m/s, V_c = 0.2m/s)$

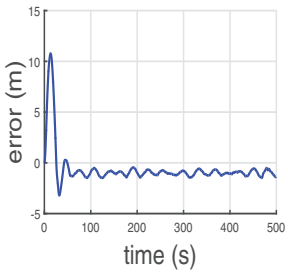

Fig. 13(b). PLOS track error

$(V_w = 3m/s, V_c = 0.2m/s)$

To evaluate the performance of the algorithms, two criteria are used. The first criterion is total cross track error D. The second criterion is total control effort U.

$$D = \sum_{t=0}^{t=T} d(t)^2$$

$$U = \sum_{t=0}^{t=T} \Delta\psi(t)^2$$

The total cross track error D and the total control effort U of the four algorithms for both situations are given in table 4.

Table 4. Total cross track error D and total control effort U

	Carrot Chasing	Nonlinear Guidance	Pure pursuit and LOS	Vector field
D (100s to 500 s) (no wind no current)	5.4	31.9	5.8	29.2
D (100s to 500 s) (wind current)	431.9	83.5	415.5	186.6
U (no wind no current)	11.4	10.4	17	5.9
U (wind current)	10.7	9.6	14.9	5.7

Since the main contribution to the total cross error was caused when the USV was in the process of turning from initialized heading angle to remove this bias from the data, the cross track error from 100s to 500s was calculated to show how much error the path following algorithm generated after the USV reached the path.

From table 4, we can see that, in terms of cross track error, when there is no wind and current, Carrot Chasing algorithm provided the most accurate results. However, when there is wind and current disturbance, nonlinear guidance algorithm provided the most stable guidance. In terms of total control effort, vector field method needs the least control effort to control the USV to follow the path, which means the USV did not always change its control command.

The characteristics of these path following algorithms can be used to deal with different mission scenarios.

CONCLUSIONS

This paper presented four common path following algorithms and their implementations in USV path following simulation.

In the simulation, nonlinear guidance path following algorithm capability performs the most accurate in the existence of current and wind disturbance. In terms of control effort, vector field algorithm needs the least control effort.

To implement the characteristics of nonlinear guidance and vector field algorithm, when the USV is in the process of avoiding static and dynamic obstacles, it might have to switch to nonlinear guidance algorithm in order to follow the path accurately and keep clear of the danger. When USV is on a long range mission or running in the open ocean, in that case accuracy is not the most important requirement, Vector field algorithm will help to improve the endurance capacity.

REFERENCES

[1] ASV Ltd. (2013). "C-Enduro LEMUSV Begins Sea Trials". Available at: http://www.asvglobal.com/latest-news/c-enduro-lemusv-begins-sea-trials. (Accessed on 11/03/2015)

[2] A. Savvaris, H. Niu, H. Oh and A. Tsourdos, "Development of Collision Avoidance Algorithms for the C-Enduro USV". The 19th World Congress. The International Federation of Automatic Control. Cape Town, South Africa. August 24-29,2014

[3] ASV Ltd. (2013). "C-Enduro Brochure". Available at: http://www.asvglobal.com/files/datasheets/c-enduro-brochure.pdf. (Accessed on 11/03/2015)

[4] A. Vasilijevic, D. Nad, N.Miskovic and Z. Vukic, "Auditory interface for teleoperation-Path following experimental results" World Congress. Vol. 19. No. 1. 2014

[5] S. Park, J. Deyst, and J. P. How, "Performance and Lyapunov stability of a nonlinear path-following guidance method," J. Guidance, Control, Dyn., vol. 30, no.6,pp. 1718-1728, 2007

[6] G. Ambrosino, M. Ariola, U. Ciniglio, F. Corraro, E. De Lellis, and A. Pironti, "Path generation and tracking in 3-D for UAVs," IEEE Trans. Control Syst. Technol., vol. 17, no. 4, pp. 980–988,2009

[7] G. Conte, S. Duranti and T. Merz, "Dynamic 3D path following for an autonomous helicopter," in Proc. 5th IFAC Symp. Intelligent Autonomous Vehicles, Oxford, U.K., pp. 473–478.

[8] M. Kothari, I. Postlethwaite and D. Gu, "A suboptimal path planning algorithm using rapidly-exploring random trees," Int. J. Aerosp. Innov., vol. 2, no. 1, pp. 93-104, 2010

[9] M. Sun, R. Zhu and X. Yang, "UAV path generation, path following and gimbal control," in Proc. IEEE Int. Conf. Networking, Sensing Control, pp. 870–873, 2008

[10] B. Wang, X. Dong and B. M. Chen, "Cascaded control of 3D path following for an unmanned helicopter," in Proc. IEEE Conf. Cybernetics Intelligent Systems, pp. 70–75, 2010

[11] C. Cao, N. Hovakimyan, I. Kaminer, V. Patel and V. Dobrokhodov. "Stabilization of cascaded systems via L1 adaptive controller with

application to a UAV path following problem and flight test results," in Proc. American Control Conf., New York, July 2007, pp. 1787–1792.

[12] D. R. Nelson, D. B. Barber, T. W. Mclain, and R. W. Beard, "Vector field path following for miniature air vehicles," IEEE Trans. Robot., vol. 23, no. 3, pp. 519–529, 2007.

[13] T.I. Fossen, "Guidance and Control of Ocean Vehicles", John Wiley & Sons Ltd, 1994